

Hyperfine structure in the $J = 1 - 0$ transitions of DCO^+ , DNC , and HN^{13}C : astronomical observations and quantum-chemical calculations

Floris F. S. van der Tak^{1,3}, Holger S. P. Müller^{2,3}, Michael E. Harding^{4,5}, and Jürgen Gauss⁴

¹ SRON Netherlands Institute for Space Research, Landleven 12, 9747 AD Groningen, The Netherlands
e-mail: vdtak@sron.nl

² I. Physikalisches Institut der Universität, Zülpicher Straße 77, 50937 Köln, Germany

³ Max-Planck-Institut für Radioastronomie, Auf dem Hügel 69, 53121 Bonn, Germany

⁴ Institut für Physikalische Chemie, Universität Mainz, 55099 Mainz, Germany

⁵ Department of Chemistry and Biochemistry, University of Texas, Austin, TX 78712, U.S.A.

Received 17 July 2009 / Accepted 27 August 2009

ABSTRACT

Context. Knowledge of the hyperfine structure of molecular lines is useful for estimating reliable column densities from observed emission, and essential for the derivation of kinematic information from line profiles.

Aims. Deuterium bearing molecules are especially useful in this regard, because they are good probes of the physical and chemical structure of molecular cloud cores on the verge of star formation. However, the necessary spectroscopic data are often missing, especially for molecules which are too unstable for laboratory study.

Methods. We have observed the ground-state ($J = 1 - 0$) rotational transitions of DCO^+ , HN^{13}C and DNC with the IRAM 30m telescope toward the dark cloud LDN 1512 which has exceptionally narrow lines permitting hyperfine splitting to be resolved in part. The measured splittings of 50–300 kHz are used to derive nuclear quadrupole and spin-rotation parameters for these species. The measurements are supplemented by high-level quantum-chemical calculations using coupled-cluster techniques and large atomic-orbital basis sets.

Results. We find $eQq = +151.12$ (400) kHz and $C_I = -1.12$ (43) kHz for DCO^+ , $eQq = 272.5$ (51) kHz for HN^{13}C , and $eQq(\text{D}) = 265.9(83)$ kHz and $eQq(\text{N}) = 288.2$ (71) kHz for DNC . The numbers for DNC are consistent with previous laboratory data, while our constants for DCO^+ are somewhat smaller than previous results based on astronomical data. For both DCO^+ and DNC , our results are more accurate than previous determinations. Our results are in good agreement with the corresponding best theoretical estimates, which amount to $eQq = 156.0$ kHz and $C_I = -0.69$ kHz for DCO^+ , $eQq = 279.5$ kHz for HN^{13}C , and $eQq(\text{D}) = 257.6$ kHz and $eQq(\text{N}) = 309.6$ kHz for DNC . We also derive updated rotational constants for HN^{13}C : $B=43545.6000(47)$ MHz and $D=93.7(20)$ kHz.

Conclusions. The hyperfine splittings of the DCO^+ , DNC and HN^{13}C $J = 1 - 0$ lines range over $0.47 - 1.28$ km s⁻¹, which is comparable to typical line widths in pre-stellar cores and to systematic gas motions on ~ 1000 AU scales in protostellar cores. We present tabular information to allow inclusion of the hyperfine splitting in astronomical data interpretation. The large differences in the ¹⁴N quadrupole parameters of DNC and HN^{13}C have been traced to differences in the vibrational corrections caused by significant non-rigidity of these molecules, particularly along the bending coordinate.

Key words. ISM: clouds – ISM: Molecules – Molecular data – Radio lines: ISM

1. Introduction

Cold interstellar clouds have long been recognized as excellent laboratories for determining basic physical quantities of molecular structure (for a review see Lemaire & Combes 2007). In particular, these clouds provide access to molecular species that are too unstable to permit sufficient terrestrial production for in-depth investigation. Some molecules were even detected in interstellar space before they were found on Earth. A classic example is the X-ogen of the early 1970's, which has gained prime importance for studying the interactions between interstellar gas and magnetic fields since its identification as HCO^+ (Buhl & Snyder 1970; Krämer & Dierksen 1976).

Astronomical observations of molecules are not only useful to provide accurate rest frequencies of spectral

lines (Pagani et al. 2001, 2009), but also to determine hyperfine parameters. The best-known case of hyperfine splitting in molecules with no unpaired electrons is the electric quadrupole splitting which occurs for nuclei with spin $I \geq 1$ such as, for example, D and ¹⁴N. A second type of splitting occurs if the molecule contains nuclei with $I > 0$ such as H, ¹³C, and ¹⁵N due to magnetic spin-rotation coupling and/or nuclear spin-nuclear spin coupling. Both effects are usually significantly smaller than the splitting due to electron spin-nuclear spin coupling in molecules with an unpaired electron and an $I > 0$ nucleus.

A recent example of astronomically determined hyperfine parameters is the determination of spectroscopic parameters of H^{13}CO^+ based on mm-wave observations of the dark cloud LDN 1512 (Schmid-Burgk et al. 2004). The exceptionally narrow lines in this cloud ($\Delta V = 0.16$ km s⁻¹) allow a frequency resolution and

accuracy that usually cannot be attained in the laboratory for short-lived molecules. This category includes molecular ions, but also radicals and reactive species such as DNC, which has a lifetime of < 1 s in the laboratory. Schmid-Burgk et al. showed that even the unresolved hyperfine splitting of ¹³CO plays a role in the case of very narrow lines. They used their spectra of LDN 1512 not only to determine the spin-rotation constant C_I of the ¹³C nucleus in H¹³CO⁺, but also to show that the magnitude of the splitting and the intensity ratio of the two resolved features depends on a much smaller effect, namely C_I of the H nucleus and the nuclear spin-nuclear spin coupling between these two nuclei (Schmid-Burgk et al. 2004).

In astrophysics, the prime use of hyperfine splitting is the possibility of measuring the optical depths of molecular lines. This fundamental quantity allows estimation of molecular column densities without assumptions about the beam filling factor. The classic example is the splitting of the NH₃ inversion lines (Ho & Townes 1983) which are used widely to measure the kinetic temperatures of dense interstellar clouds (Walmsley & Ungerechts 1983). In addition, knowledge of hyperfine structure is essential for deriving the kinematic structure of clouds from observations of molecular line profiles. In particular, the central regions of pre-stellar cores are currently of great interest, as the places where the transition from spherical infall to disk-like rotation occurs (Bergin & Tafalla 2007). However, in these objects, many 'standard' kinematic probes are unavailable due to freeze-out onto dust grains (Bergin et al. 2002). Deuterium bearing molecules are abundant even under these conditions, but their lines always exhibit hyperfine splitting due to the nonzero spin ($I = 1$) of the D nucleus. For example, Van der Tak et al. (2005) used observations of H₂D⁺ to study the kinematics at the center of the pre-stellar core LDN 1544, where most other molecules are frozen onto dust grains.

In the laboratory, the Doppler-limited line widths in the 3 mm region are of the order of 200 kHz, making it possible to resolve moderate to large hyperfine splitting. However, very small quadrupole splitting, such as the ¹⁴N splitting in HNC or essentially all of the deuterium quadrupole splitting cannot be resolved in this frequency region. Sub-Doppler resolution techniques, such as Lamb-dip spectroscopy or molecular beam millimeter-wave Fourier transform spectroscopy, are sometimes available, but the former is usually not feasible for short-lived species, and the latter type of measurements is available only in very few laboratories.

While the relatively large nitrogen quadrupole splitting of DCN has been resolved in the laboratory (Brünken et al. 2004) and in space (Turner 2001), the hyperfine structure of the astrophysically important DCO⁺, HN¹³C and DNC species had not yet been resolved at the time of our observations (2004-2005). High-resolution spectroscopy of these species is not only astronomically useful to determine the optical depths of the lines, but also to verify the results of quantum-chemical calculations of spectroscopic constants. For example, Frerking et al. (1979) measured a nitrogen quadrupole moment of 0.28 (3) MHz for HNC in the dark cloud LDN 134N. Even though this value

is not particularly accurate, it is in good agreement with the very recent, more accurate laboratory value of 0.2645 (46) MHz (Bechtel et al. 2006). More recently, Caselli et al. (1995) determined hyperfine parameters for the N₂H⁺ $J = 1 - 0$ line from astronomical data, which Gerin et al. (2001) extended to higher- J transitions, and Dore et al. (2004) to the N₂D⁺ isotopologue. This paper describes a new determination of the hyperfine structure of the $J = 1 - 0$ lines of DCO⁺, DNC and HN¹³C, based on observations of LDN 1512. The measurements are supplemented by high-level quantum-chemical calculations of the corresponding hyperfine parameters using state-of-the-art coupled-cluster techniques together with large atomic-orbital basis sets.

2. Observations

Observations of the $J = 1 - 0$ lines of DCO⁺, DNC and HN¹³C near 72039, 76306 and 87091 MHz were performed on 2004 August 5 – 6, and 2005 March 12 and July 29. The 30-m telescope of the Institut de Radio Astronomie Millimétrique (IRAM)¹ was used, with the facility receivers A100 and B100 as front end. The tuning range of these receivers had just been extended from 80 GHz down to 70 GHz. The beam size is 33'' in this frequency range, and the main beam efficiency is $\approx 80\%$. We used the Versatile Spectral Assembly (VESPA) correlator as backend to achieve a spectral resolution of 3.3 kHz, or 0.013 km s⁻¹. Sideband gain ratios, measured with the Martin-Puplett interferometer, were in the range 0.91–1.13, depending on backend module. System temperatures were ≈ 300 K at 72 GHz, ≈ 200 K at 76 GHz and ≈ 150 K at 87 GHz. Integration times were 78 minutes (on+off) at 72 GHz, 215 minutes at 76 GHz and 197 minutes at 87 GHz, giving rms noise levels of $T_{\text{MB}} = 158$ mK at 72 GHz, 47 mK at 76 GHz and 41 mK at 87 GHz. Pointing was checked every hour on the nearby planet Venus.

The position observed is $\alpha = 05:00:54.40$, $\delta = +32:39:37.0$ (B1950). The cloud velocity at this position, as determined from observations of the HC₃N 3–2 line near 27294 MHz with the Effelsberg 100-m telescope², is $V_{\text{LSR}} = 7.069 \pm 0.001$ km s⁻¹. The beam size of the 100-m telescope at the HC₃N frequency is almost equal to that of the 30-m telescope at the DCO⁺, DCN and DNC frequencies, so the effect of the known velocity gradients within the LDN 1512 cloud should be very small. An upper limit is obtained by convolving the HC₃N data to a 50'' beam, which gives a velocity of $V_{\text{LSR}} = 7.063 \pm 0.001$ km s⁻¹. Therefore the effect of the velocity gradient in LDN 1512 is less than 0.006 km s⁻¹. For further discussion of these velocity gradients and for accurate HC₃N frequencies, see Schmid-Burgk et al. (2004).

The data reduction was performed using the Continuum and Line Analysis Single-dish Software (CLASS) pack-

¹ IRAM is an international institute for research in millimeter astronomy, co-funded by the Centre National de la Recherche Scientifique (France), the Max Planck Gesellschaft (Germany) and the Instituto Geografico Nacional (Spain).

² The Effelsberg telescope is operated by the Max-Planck-Institut für Radioastronomie

age³ and followed standard procedures, except that the combination of data taken on different epochs posed unusual challenges. The telescope system corrects the frequency scale of the spectra for heliocentric motion of the Earth, but the correction is only exact for the center of the receiver bandpass. In our case, the HN¹³C line was observed at an offset of 160 MHz to allow simultaneous observation of other lines. The telescope system adds this offset as an absolute value, but the orbital motion of the Earth actually dilates or shrinks the frequency scale by a factor of $\sim 10^{-4}$, the ratio of the telluric orbital velocity and the velocity of light. The HN¹³C spectra were taken 121 days apart, and the frequency shift is $16\text{ kHz} \times \cos \delta$, where δ is the ecliptic latitude of the source (10°). Indeed, the two HN¹³C spectra agree very well after a shift of 21 kHz, and similarly, the DNC spectra are consistent with the expected shift of 4.4 kHz for an epoch separation of 340 days. To obtain the correct absolute frequency scale, the spectra of all epochs were shifted to a hypothetical observing date of June 8, which is the day in the year that the Sun and LDN 1512 have the same hour angle and transit at the same time. We assume the frequency accuracy to be 3 kHz. This is about twice the LSR velocity gradient of the source and leaves some room for possible errors in the correction of the heliocentric motion.

3. Quantum-chemical calculations

High-level quantum-chemical calculations using coupled-cluster (CC) techniques (Čížek 1966a,b; Gauss 1998; Crawford & Schaefer 2000; Bartlett & Musiał 2007) have been performed for the hyperfine parameters of DCO⁺, HN¹³C, and DNC. Calculations have been carried out for the most part at the CC singles and doubles (CCSD) level (Purvis & Bartlett 1982) augmented by a perturbative treatment of triple excitations (CCSD(T); Raghavachari et al. 1989) which has proven in many cases to provide a reliable account of electron-correlation effects on energies and properties. The required one-particle basis sets for these calculations have been taken from Dunning's hierarchy of correlation-consistent basis sets with cc-pVXZ denoting the standard valence sets (Dunning 1989), cc-pCVXZ those with additional core-polarizing functions (Woon & Dunning 1995), and aug-cc-p(C)VXZ those with additional diffuse functions (Kendall et al. 1992). Here, X represents the cardinal number of the basis sets and values of 3 (= T), 4 (= Q), and 5 have been chosen in the present work.

The theoretical determination of quadrupole coupling constants is based on the evaluation of the electric-field gradients (efgs) at the corresponding nuclei. The nuclear quadrupole moments required to convert the efgs to the quadrupole couplings are taken from the literature (Pyykkö 2008), and the following values have been here adopted: 2.860 (15) mbarn for D and 20.44 (3) mbarn for ¹⁴N. The reported calculations also take into account zero-point vibrational effects on the quadrupole couplings. Those are treated in a perturbative manner as described in Auer et al. (2003) and necessitate the evaluation of quadratic and cubic force

fields. The latter are obtained using analytic second-derivative techniques (Gauss & Stanton 1997) as described in Stanton & Gauss (2000). Spahn et al. (2008) provide recent examples of the very good agreement between experiment and calculations for DC₃N and HC₃N.

The nuclear spin-rotation tensor is a second-order response property and can be computed via the associated second derivative of the energy with respect to nuclear spin and the rotational angular momentum as perturbations. As described in Gauss et al. (1996), we calculate the spin-rotation tensor using perturbation-dependent basis functions (so-called rotational London atomic orbitals) in order to ensure fast basis-set convergence. No vibrational averaging has been performed for the spin-rotation tensors, as the corresponding theoretical expressions exhibit numerical problems in the case of polyatomic linear molecules.

To ensure convergence in the electron-correlation treatment, a few calculations have been performed at levels beyond CCSD(T), i.e. at the CCSDT level (Noga & Bartlett 1987; Scuseria & Schaefer 1988) with a full treatment of triple excitations and at the CCSDTQ level (Kállay & Surján 2001; Kállay et al. 2004) with an additional consideration of quadruple excitations.

All calculations have been carried out using the CFour quantum-chemical program package⁴. Only the CCSDT and CCSDTQ calculations have been carried out with the MRCC package⁵ which has been interfaced to CFour.

Tables 1 and 2 summarize our computational results for the hyperfine parameters of DCO⁺, HN¹³C, and DNC and in particular document the convergence of the calculated values with respect to basis set and electron-correlation treatment.

4. Results

4.1. Hyperfine splitting of DCO⁺

Figure 1 shows the DCO⁺ spectrum toward LDN 1512. The spin $I = 1$ of the D nucleus splits the transition into three components, labeled by the total angular momentum $F = J + I$. The three expected hyper-

⁴ Coupled Cluster techniques for Computational Chemistry, a quantum-chemical program package by J. F. Stanton, J. Gauss, M. E. Harding, and P. G. Szalay with contributions from A. A. Auer, R. J. Bartlett, U. Benedikt, D. E. Bernholdt, C. Berger, Y.J. Bomble, O. Christiansen, M. Heckert, O. Heun, C. Huber, D. Jonsson, J. Jusélius, K. Klein, W. J. Lauderdale, D. Matthews, T. Metzroth, D. P. O'Neill, D. R. Price, E. Prochnow, K. Ruud, F. Schiffmann, S. Stopkowitz, M. E. Varner, J. Vázquez, J. D. Watts, F. Wang and the integral packages MOLECULE (J. Almlöf and P. R. Taylor), PROPS (P. R. Taylor), ABACUS (T. Helgaker, H. J. Aa. Jensen, P. Jørgensen, and J. Olsen), and ECP routines by A. V. Mitin and C. van Wüllen. For the current version, see <http://www.cfour.de>

⁵ MRCC, a string-based quantum chemical program suite written by M. Kállay. See <http://www.mrcc.hu>

³ <http://www.iram.fr/IRAMFR/GILDAS>

fine components are clearly detected and resolved. We derive the frequencies of these components by fitting three independent Gaussians to the observed spectrum. The fit uses a cloud velocity of $V_{\text{LSR}} = 7.069 \text{ km s}^{-1}$ (see § 2) and a line width of 35 kHz which is the average width of the three components. The spacings of the components, independent of V_{LSR} , are -0.198 (6) and $+0.269$ (6) km s^{-1} which is $+47.58$ (144) and -64.64 (144) kHz (Table 3). These splittings are linear combinations of the quadrupole coupling constant eQq and the spin-rotation constant C_I of the D nucleus (e.g., Townes & Schawlow 1955). Solving the two equations with two unknowns gives the eQq and C_I values given in Table 4.

The present value of C_I in Table 4 is smaller in magnitude than that by Caselli & Dore (2005) while eQq is larger. However, agreement exists within the larger uncertainties from Caselli & Dore (2005). These authors also observed the LDN 1512 cloud with the IRAM 30m telescope, but at a different position, where the lines are weaker. Therefore, the signal-to-noise ratio of their spectra is lower, even though the integration time has been longer.

The quantum-chemical calculations for DCO⁺ (see Table 1) yield as best values for eQq 156.0 kHz (CCSD(T)/cc-pCV5Z calculations plus vibrational corrections); the small changes from the quadruple-zeta (QZ) to the quintuple-zeta (5Z) basis set suggests a minute increase of probably less than 1 kHz upon extrapolation to the basis-set limit. The agreement is good, within twice the experimental uncertainties, for the fit in which C_I has been varied. The agreement is slightly worse for the fit in which C_I was kept fixed to the quantum-chemically calculated value and slightly worse still in comparison to the previous values from Caselli & Dore (2005), see Table 4.

The best theoretical value for C_I is -0.69 kHz. As discussed in § 3, no vibrational corrections could be computed for this value. However, since the vibrational correction to eQq is fairly small, it is likely that the one on C_I will be small also, possibly of order of 0.1 kHz. The convergence patterns seen in Table 2 suggest that remaining errors in the calculations can be considered rather small so that we conclude, based on these theoretical estimates as well as the results of our measurements that Caselli & Dore (2005) overestimated C_I due to the limited signal-to-noise in their spectrum. Both fitted values agree within the fairly large uncertainties with the theoretical value.

The absolute positions of the strongest hyperfine component from the present astronomical observations agree to about 3 kHz with the previous observation (Caselli & Dore 2005).

4.2. Anomalous excitation of DCO⁺

The continuous line in Figure 1 is a model fit to the data that uses the splitting constants that we just derived. The model was computed with the hyperfine structure (HFS) routine within CLASS. This routine assumes that the

hyperfine components of the transition have the same width and the same excitation temperature. While the data support the first assumption, the second apparently does not hold. The highest-frequency $F = 1 - 1$ component has a higher intensity than the model predicts. Such ‘hyperfine anomalies’ are well-known for the $J = 1 - 0$ line of HCN, where the $F = 0 - 1$ component is unexpectedly strong toward many dark clouds (e.g., Walmsley et al. 1982). The implied difference in excitation temperatures between the hyperfine components can be understood through detailed calculations of hyperfine selective collisional cross sections (Monteiro & Stutzki 1986). Such calculations do not exist for DCO⁺ at present, although they have been reported for N₂H⁺ (Daniel et al. 2005), where a similar excitation anomaly has been observed (Caselli et al. 1995). Hyperfine selective collision data for the electron impact excitation of HCN, HNC, DCN and DNC are presented by Faure et al. (2007), but do not apply here, since the electron abundance in dark clouds is low.

4.3. Hyperfine splitting of DNC

Figure 2 shows the spectrum of DNC toward LDN 1512. The profile consists of one weak, isolated component at low frequency, and two stronger, broader peaks which appear to be blends of several components. The spins $I = 1$ of the D and ¹⁴N nuclei lead theoretically to a splitting into nine components at seven different frequencies, but not all these components are resolved in the current data. Since the hyperfine splitting of both nuclei are of similar magnitude, we have used the symmetric coupling scheme $I_{\text{tot}} = I_{\text{N}} + I_{\text{D}}$ and $F = J + I_{\text{tot}}$. In contrast, Bechtel et al. (2006) use the sequential coupling scheme, which only affects the labeling of the levels, but not the shape of the hfs pattern. The isolated component is well fitted with a Gaussian profile of width 0.150 (1) km s^{-1} . We have fitted the profile with an ‘empirical’ model consisting of several Gaussians with independent positions and intensities, but with the width fixed to 0.15 km s^{-1} . The fit has significant residuals if four or five Gaussians are used, but the sum of six Gaussians (plus one for the isolated feature) gives a satisfactory fit to the observed profile (Fig. 2a).

The results of the empirical model are in good agreement with our quantum-chemical calculations, which predict seven hyperfine components for this transition, due to the nuclear spin of both D and N. In the case of DNC, the quadrupole moments eQq of the D and N nuclei are similar in magnitude, unlike in DCN where $eQq(\text{N}) \gg eQq(\text{D})$.

The positions of the components of the empirical model are in good agreement with the predictions based on quantum-chemical calculations, except for the highest-frequency component. Suspecting that this mismatch is caused by the small separation of the $2,2 \rightarrow 2,2$ and the (coinciding) $0,1 \rightarrow 0,0$ and $0,1 \rightarrow 2,2$ components, we have reduced the empirical model to five Gaussians, and freed up the width of the fourth Gaussian, which represents these components. This ‘semi-empirical’ model gives an excellent match to the data, as shown by the solid line in Fig. 2b. The width of the fourth Gaussian

is 0.202 (9) km s⁻¹ implies a separation of the 2,2→2,2 component from the 0,1→0,0 and 0,1→2,2 components of 0.05 km s⁻¹. This result is in good agreement with the theoretical results: the calculated splitting is 8.7 kHz, but the apparent separation is smaller because of the small intensity of the 0,1→0,0 and 0,1→2,2 components; see Table 3.

The hyperfine parameters determined for DNC are compared in Table 5 with those previously determined in the laboratory by Bechtel et al. (2006) and with the best ab initio values. We note a good agreement between the two experimental sets of data, but emphasize that our values have reduced error bars. The comparison with the theoretical best estimates is also favorable and lends support to the reliability of the experimentally determined hyperfine parameters. The theoretical quadrupole coupling terms determined with the largest basis set and incorporating vibrational corrections are 257.6 and 309.6 kHz for the D and ¹⁴N nucleus, respectively, while the calculated nitrogen spin-rotation constant amounts to 5.54 kHz. The theoretical values are apparently slightly closer to the previous values (Bechtel et al. 2006). While a smooth and fast convergence is observed in the calculation of the spin-rotation and deuterium quadrupole coupling constants, the determination of the nitrogen quadrupole coupling constant turned out to be challenging. Going from the quadruple-zeta to the quintuple-zeta set causes a change of 16 kHz and vibrational corrections amount to more than 40 kHz, while electron-correlation effects beyond CCSD(T) are found to be less important. However, the noted problems in the accurate determination of the nitrogen quadrupole coupling constant can be traced back to the smallness of the actual value which is roughly one order of magnitude smaller than the corresponding quadrupole coupling in DCN (Brünken et al. 2004). Moreover, the changes in the calculated eQq values decrease fairly rapidly by a factor of about 6 with increasing size of the basis set. Taking into account the decrease in the magnitude of the vibrational corrections one can estimate a value of about 306.5 ± 1 kHz as the CCSD(T) value at the infinitely large basis set, in agreement within the uncertainty of the laboratory value and within 2.5 times the uncertainties of the present astronomical observations.

The absolute positions of the isolated hyperfine components from the present astronomical observations agree to 1 kHz with the previous laboratory frequencies (Bechtel et al. 2006). The laboratory frequency was deemed to be uncertain to 5 kHz while our astronomical frequency is uncertain to probably no more than 3 kHz.

4.4. Hyperfine splitting of HN¹³C

Figure 3 shows the spectrum of HN¹³C $J = 1 - 0$ toward LDN 1512. One weak, isolated hyperfine feature at low frequency (LF for short) as well as two somewhat resolved ones can be recognized easily as would be expected for a molecule with a ¹⁴N nucleus. Analyses of the astronomical spectrum as well as simulations of the spectrum based on the experimental quadrupole moment (eQq) for HNC (Bechtel et al.

2006), the quantum-chemically calculated nuclear spin-rotation parameters (C_I) and the spin-spin coupling terms (S_{XY}) derived from the interatomic distances and the nuclear magnetic moments reveal that the situation is more complicated. First, contributions from the ¹³C nucleus considerably broaden the central hyperfine feature (CF for short) such that a shoulder to the lower frequency side should be discernable. Second, the hyperfine pattern should get wider, and the relative intensity of the highest frequency feature (HF for short) should increase somewhat with respect to the central one. Splitting caused by the H nucleus increases the total number of hyperfine components further, but the total number of observable features does not increase. However, it is noteworthy that the H hyperfine parameters counteract somewhat the effects caused by the ¹³C nucleus mentioned under "second". The net effect is one isolated, weak hyperfine feature at low frequencies, one strong and very broad CF with a low-frequency shoulder, and a HF that should be stronger than the isolated component, but weaker than the central one.

Analyses were started assuming three different hyperfine features with three different widths. The LF-HF splitting seemed reasonable, but the HF was too strong compared with the CF, and the position of the CF was too low in frequency. Fitting two features for the CF required their width to be equal to that of the LF which was determined to be 43 kHz as expected from the simulations. A fit of four components with widths of 43 kHz was still fairly poor. Simulations suggested the width of the HF to be about 15 % larger than that of the remaining components. The analysis of the astronomical spectrum improved somewhat, but was still not satisfactory. Moreover, a fit of eQq to the splittings with all other hyperfine parameters kept fixed yielded a value of 272.5 ± 5.1 kHz, which is larger than the one determined for HNC, 264.5 ± 4.6 kHz, in the laboratory (Bechtel et al. 2006), but in agreement within the quoted uncertainties. The rms of the fit is 5.1 kHz. Releasing the width of the HF gave the best analysis of the astronomical spectrum, but yielded a width of 71.5 ± 2.3 kHz, much bigger than expected from the simulations. The spectroscopic fit yields $eQq = 258.7 ± 5.1$ kHz, which is now smaller than the HNC value, but again in agreement within uncertainties. The rms of the fit is, with 4.0 kHz, slightly better than the fit mentioned before (Table 3).

The contributions to the hyperfine splittings decrease from ¹⁴N over ¹³C to H. Therefore, we apply a sequential coupling scheme: $F_1 = J + I(^{14}\text{N})$; $F_2 = J + I(^{13}\text{C})$; $F = J + I(\text{H})$. Only eQq could be determined for the ¹⁴N nucleus. Trial fits with $C(^{14}\text{N})$ or $C(^{13}\text{C})$ or both released yielded values for these parameters that were deemed to be unreliable as they could differ by as much as about 5 kHz from the predicted values.

The final values for the hyperfine parameters for HN¹³C are given in Table 6. The resulting nitrogen quadrupole coupling of 272.5 (51) kHz is in good agreement with the best theoretical value of 279.5 kHz, in particular when noting the slow basis-set convergence in the corresponding calculations. The vibrational contributions are much larger still than the already large contributions for DNC; they amount to about 46 kHz for HN¹³C. These contributions decrease again slightly in magnitude going from the quadruple-zeta to the quintuple-zeta basis

set. Thus, the CCSD(T) $eQq(^{14}\text{N})$ value at the basis-set limit is probably around 3 kHz smaller than the one calculated at the cc-pCV5Z basis set with vibrational corrections and now agreeing within the uncertainty with the value from astronomical observations.

4.5. Rotational and distortion parameters for HN¹³C

Accurate rotational as well as distortion parameters are available for DNC (Brünken et al. 2006; Bechtel et al. 2006) and DCO⁺ (Caselli & Dore 2005; Lattanzi et al. 2007) and the present measurements will only modify these parameters slightly. In contrast, only sparse data are available for HN¹³C. Pearson et al. (1976) measured the $J=1\leftarrow 0$ and $2\leftarrow 1$ rotational transitions of several HNC isotopologs. More recently, Maki & Mellau (2001) obtained rovibrational transitions of the ν_2 bending mode of HN¹³C together with extensive data for HNC. Replacing the $J=1\leftarrow 0$ laboratory rest frequency with our astronomical rest frequency (Table 3) reduces the uncertainties of B and D by factors of 5 and 1.7, respectively. Fixing H to a value of 157 mHz taken from HNC (Thorwirth et al. 2000; Bechtel et al. 2006), we obtain $B = 43545.6000$ (47) MHz and $D = 93.7$ (20) kHz; the numbers in parentheses are one standard deviation in units of the least significant figures. The present values of B and D agree with the previous ones within their larger uncertainties (Pearson et al. 1976). The resulting predictions are accurate up to ≈ 500 GHz but should be viewed with some caution at higher frequencies.

5. Discussion and conclusions

5.1. Astronomical implications

At spectral resolutions of ~ 0.1 km s⁻¹, as commonly achieved by astronomical instrumentation in the 3 mm wavelength range, the $J = 1-0$ line of DCO⁺ splits into three hyperfine components, the HN¹³C $J = 1-0$ line into four, and the DNC $J = 1-0$ line into six. Table 7 gives the velocity offsets and the relative strengths of these components. The strengths are theoretical values which only apply if the lines are optically thin and the excitation is thermalized; as Section 4.2 discusses, these conditions are often not fulfilled, so that detailed radiative transfer modeling is needed to extract physical information out of the observed hyperfine intensities.

The hyperfine splitting extends over 0.47 km s⁻¹ for DCO⁺, over 1.28 km s⁻¹ for DNC, and over 0.73 km s⁻¹ for HN¹³C. These intervals are comparable to or larger than the total (thermal + turbulent) line widths in many astrophysical objects, in particular pre- and protostellar cores in star-forming regions (Bergin & Tafalla 2007). Taking these splittings into account is therefore crucial to derive accurate column densities of DCO⁺, DNC and HN¹³C from their ground-state rotational lines.

The magnitude of the hyperfine splittings is also comparable to the velocities of infalling, outflowing and rotational motions around protostars on ~ 1000 AU scales

(e.g., Hogerheijde 2001). Taking the splitting into account is therefore essential for a correct determination of the velocity field of the gas from these lines. The quadrupole splittings of linear molecules decrease rapidly with increasing J , at least for the strong transitions, so that going to higher- J lines would seem a way to avoid this complication. However, at the typical (low) temperatures and densities of pre- and protostellar cores, the higher- J lines of DCO⁺, DNC and HN¹³C are usually less excited and thus weaker than the ground-state lines.

5.2. Molecular physics implications

The most remarkable aspect of the present results from the molecular physics point of view are the large vibrational corrections to the ¹⁴N eQq values of HN¹³C and DNC and the corresponding large differences in the ground state eQq values. Isotopic differences in experimentally determined quadrupole coupling constants are usually not or barely significant. Significant effects have been observed e.g. by Gatehouse et al. (1998) where ¹⁰B/¹¹B isotopic shifts of around 15 kHz were determined for quadrupole coupling constants of both ³⁵Cl and ³⁷Cl of CIBO, though these shifts were only very small fractions ($< 10^{-3}$) of the constants themselves. The authors attributed these effects to the non-rigidity of the molecule in particular along the bending coordinate. Experimental work (Bechtel et al. 2008) and calculations (Wong 2008) lend support to this view and suggest that low-order vibrational corrections to the eQq values are probably not sufficient for very accurate predictions of quadrupole coupling constants for specific vibrational states.

While the bending mode of HNC is known to be fairly non-rigid, those of the isoelectronic HCN, HCO⁺, and N₂H⁺ molecules are much more rigid. However, the bending mode of the HOC⁺ molecule is even less rigid than that of HNC. Therefore, it would be interesting to investigate the ¹⁷O quadrupole coupling constants of H¹⁷OC⁺ and D¹⁷OC⁺. The HOC⁺ molecule is less abundant than its isomer HCO⁺ by factors of ~ 100 in diffuse clouds and ~ 1000 in dense clouds (Liszt et al. 2004), but HOC⁺ is strongly enhanced in regions with strong radiation fields and/or shocks (Rizzo et al. 2003; Fuente et al. 2005, 2008), so these may be good places to search for its rare isotopologues. In addition, this molecule is not so easy to produce in the laboratory. Thus, the easiest way to obtain information on the hyperfine structure of this ion are detailed quantum-chemical calculations.

New or updated predictions of the rotational spectra for DCO⁺, DNC, and HN¹³C will be available in the catalog section of the Cologne Database for Molecular spectroscopy⁶ (Müller et al. 2001, 2005).

Acknowledgements. The authors thank Michael Grewing (IRAM) for awarding Director's Time to our observing project, Johannes Schmid-Burgk (MPIfR) for discussions about the LDN 1512 cloud, Gabriel Paubert (IRAM) for discussions on heliocentric corrections, and Arnaud Belloche and Dirk Muders (MPIfR) for assistance with the

⁶ website: <http://www.astro.uni-koeln.de/cdms/>

observations. H.S.P.M. thanks the Deutsche Forschungsgemeinschaft (DFG) for initial support through the collaborative research grant SFB 494. He is grateful to the Bundesministerium für Bildung und Forschung (BMBF) for recent support which was administered by the Deutsches Zentrum für Luft- und Raumfahrt (DLR). M.E.H. and J.G. acknowledge support from the Deutsche Forschungsgemeinschaft (DFG) and the Fonds der Chemischen Industrie.

References

- Auer, A. A., Gauss, J., & Stanton, J. F. 2003, *J. Chem. Phys.*, 118, 10407
- Bartlett, R. J. & Musial, M. 2007, *Rev. Mod. Phys.*, 79, 291
- Bechtel, H. A., Steeves, A. H., & Field, R. W. 2006, *ApJ*, 649, L53
- Bechtel, H. A., Steeves, A. H., Wong, B. M., & Field, R. W. 2008, *Angew. Chem.*, 120, 3011
- Bergin, E. A., Alves, J., Huard, T., & Lada, C. J. 2002, *ApJ*, 570, L101
- Bergin, E. A. & Tafalla, M. 2007, *ARA&A*, 45, 339
- Brünken, S., Fuchs, U., Lewen, F., et al. 2004, *J. Mol. Spectrosc.*, 225, 152
- Brünken, S., Müller, H. S. P., Thorwirth, S., Lewen, F., & Winnewisser, G. 2006, *J. Mol. Struct.*, 780, 3
- Buhl, D. & Snyder, L. E. 1970, *Nature*, 228, 267
- Caselli, P. & Dore, L. 2005, *A&A*, 433, 1145
- Caselli, P., Myers, P. C., & Thaddeus, P. 1995, *ApJ*, 455, L77
- Crawford, T. D. & Schaefer, H. F. I. 2000, *Rev. Comp. Chem.*, 14, 33
- Daniel, F., Dubernet, M.-L., Meuwly, M., Cernicharo, J., & Pagani, L. 2005, *MNRAS*, 363, 1083
- Dore, L., Caselli, P., Beninati, S., et al. 2004, *A&A*, 413, 1177
- Dunning, T. H. J. 1989, *J. Chem. Phys.*, 90, 1007
- Faure, A., Varambhia, H. N., Stoecklin, T., & Tennyson, J. 2007, *MNRAS*, 382, 840
- Frerking, M. A., Wilson, R. W., & Langer, W. D. 1979, *ApJ*, 232, L65
- Fuente, A., García-Burillo, S., Gerin, M., et al. 2005, *ApJ*, 619, L155
- Fuente, A., García-Burillo, S., Usero, A., et al. 2008, *A&A*, 492, 675
- Gatehouse, B., Müller, H. S. P., & Gerry, M. C. L. 1998, *J. Mol. Spectrosc.*, 190, 157
- Gauss, J. 1998, in *Encyclopedia of Computational Chemistry*, edited by P.v.R. Schleyer et al. (Wiley, New York), 615
- Gauss, J., Ruud, K., & Helgaker, T. 1996, *J. Chem. Phys.*, 105, 2804
- Gauss, J. & Stanton, J. F. 1997, *Chem. Phys. Lett.*, 276, 70
- Gerin, M., Pearson, J. C., Roueff, E., Falgarone, E., & Phillips, T. G. 2001, *ApJ*, 551, L193
- Ho, P. T. P. & Townes, C. H. 1983, *ARA&A*, 21, 239
- Hogerheijde, M. R. 2001, *ApJ*, 553, 618
- Kállay, M., Gauss, J., & Szalay, P. G. 2004, *J. Chem. Phys.*, 119, 2991
- Kállay, M. & Surján, P. R. 2001, *J. Chem. Phys.*, 115, 2945
- Kendall, R. A., Dunning, T. H. J., & Harrison, R. J. 1992, *J. Chem. Phys.*, 96, 6796
- Krämer, W. P. & Diercks, G. H. F. 1976, *ApJ*, 205, L97
- Lattanzi, V., Walters, A., Drouin, B. J., & Pearson, J. C. 2007, *ApJ*, 662, 771
- Lemaire, J. L. & Combes, F., eds. 2007, *Molecules in Space and Laboratory*, proceedings of the meeting held in Paris, May 14–18, 2007; *Astrophysique Moléculaire Publications*, S. Diana, 2007
- Liszt, H., Lucas, R., & Black, J. H. 2004, *A&A*, 428, 117
- Maki, A. G. & Mellau, G. C. 2001, *J. Mol. Spectrosc.*, 206, 47
- Monteiro, T. S. & Stutzki, J. 1986, *MNRAS*, 221, 33P
- Müller, H. S. P., Schlöder, F., Stutzki, J., & Winnewisser, G. 2005, *J. Mol. Struct.*, 742, 215
- Müller, H. S. P., Thorwirth, S., Roth, D. A., & Winnewisser, G. 2001, *A&A*, 370, L49
- Noga, J. & Bartlett, R. J. 1987, *J. Chem. Phys.*, 86, 7041
- Pagani, L., Daniel, F., & Dubernet, M.-L. 2009, *A&A*, 494, 719
- Pagani, L., Gallego, A. T., & Apponi, A. J. 2001, *A&A*, 380, 384
- Pearson, E. F., Creswell, R. A., Winnewisser, M., & Winnewisser, G. 1976, *Z. Naturforsch. A*, 31, 221
- Purvis, III, G. D. & Bartlett, R. J. 1982, *J. Chem. Phys.*, 76, 1910
- Pyykkö, P. 2008, *Mol. Phys.*, 106, 1965
- Raghavachari, K., Trucks, G. W., Pople, J. A., & Head-Gordon, M. 1989, *Chem. Phys. Lett.*, 157, 479
- Rizzo, J. R., Fuente, A., Rodríguez-Franco, A., & García-Burillo, S. 2003, *ApJ*, 597, L153
- Schmid-Burgk, J., Muters, D., Müller, H. S. P., & Brupbacher-Gatehouse, B. 2004, *A&A*, 419, 949
- Scuseria, G. E. & Schaefer, H. F. I. 1988, *Chem. Phys. Lett.*, 152, 382
- Spahn, H., Müller, H. S. P., Giesen, T. F., et al. 2008, *Chemical Physics*, 346, 132
- Stanton, J. F. & Gauss, J. 2000, *Int. Rev. Phys. Chem.*, 19, 61
- Thorwirth, S., Müller, H. S. P., Lewen, F., Gendriesch, R., & Winnewisser, G. 2000, *A&A*, 363, L37
- Townes, C. H. & Schawlow, A. L. 1955, *Microwave Spectroscopy* (New York: McGraw-Hill)
- Turner, B. E. 2001, *ApJS*, 136, 579
- Čížek, J. 1966a, *Adv. Chem. Phys.*, 14, 35
- Čížek, J. 1966b, *J. Chem. Phys.*, 45, 4256
- Van der Tak, F. F. S., Caselli, P., & Ceccarelli, C. 2005, *A&A*, 439, 195
- Walmsley, C. M., Churchwell, E., Nash, A., & Fitzpatrick, E. 1982, *ApJ*, 258, L75
- Walmsley, C. M. & Ungerechts, H. 1983, *A&A*, 122, 164
- Wong, B. M. 2008, *Phys. Chem. Chem. Phys.*, 10, 5599
- Woon, D. E. & Dunning, T. H. J. 1995, *J. Chem. Phys.*, 103, 4572

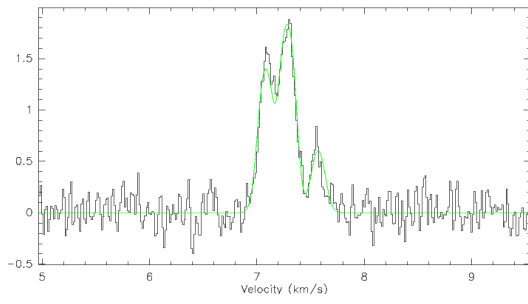


Fig. 1. Spectrum of the $J = 1 - 0$ transition of DCO⁺ toward the dark cloud LDN 1512, obtained with the IRAM 30m telescope. Vertical scale is antenna temperature (T_{mb}) in K. Overplotted is a model fit which assumes that the three hyperfine components have the same width and excitation temperature.

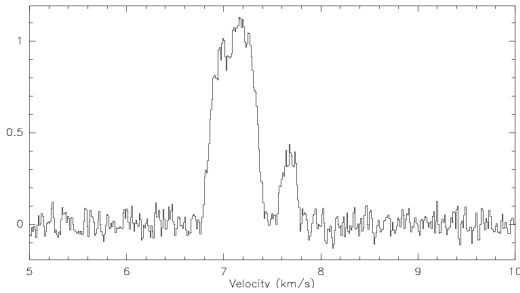


Fig. 3. Spectrum of the $J = 1 - 0$ transition of HN¹³C toward the dark cloud LDN 1512, obtained with the IRAM 30m telescope. Vertical scale is antenna temperature (T_{mb}) in K.

Table 1. Computed quadrupole-coupling constants eQq (kHz) for DCO⁺, HN¹³C, and DNC.^a

Computational level	DCO ⁺		HN ¹³ C		DNC	
	D	N	D	N	D	N
CCSD/cc-pCVDZ			308.6	1009.5		
CCSD(T)/cc-pCVDZ			309.3	1021.4		
CCSDT/cc-pCVDZ			309.3	1029.1		
CCSDTQ/cc-pCVDZ			309.2	1033.2		
CCSD(T)/cc-pCVTZ			290.8	431.9		
CCSD(T)/cc-pCVQZ	159.2	341.6	279.8	341.6		
CCSD(T)/cc-pCVQZ + vib	153.6	294.8	259.1	325.2		
CCSD(T)/cc-pCV5Z	162.2	325.5	278.3	325.5		
CCSD(T)/cc-pCV5Z + vib	156.0	279.5	257.6	309.6		

^a All calculations have been performed at geometries obtained at the same computational level.

Table 2. Computed nuclear spin-rotation constants C_I (kHz) for DCO⁺, HN¹³C, and DNC.^a

Computational level	DCO ⁺		HN ¹³ C			DNC	
	D	H	N	C	D	N	
CCSD(T)/cc-pCVTZ	-0.701	-4.551	22.954	6.194	-0.611	5.417	
CCSD(T)/cc-pCVQZ	-0.695	-4.505	23.345	6.292	-0.605	5.502	
CCSD(T)/cc-pCV5Z	-0.693	-4.486	23.471	6.330	-0.602	5.536	
CCSD(T)/aug-cc-pVTZ	-0.700	-4.575	22.878	6.200	-0.614	5.423	
CCSD(T)/aug-cc-pVQZ	-0.695	-4.510	23.318	6.295	-0.605	5.505	
CCSD(T)/aug-cc-pV5Z	-0.693	-4.486	23.456	6.331	-0.602	5.537	

^a The calculations have been performed at geometries obtained at the CCSD(T)/cc-pCVQZ level of theory (DCO⁺: $r(\text{CO}) = 1.10639 \text{ \AA}$, $r(\text{HC}) = 1.09236 \text{ \AA}$; HN¹³C, DNC: $r(\text{NC}) = 1.16927 \text{ \AA}$, $r(\text{HN}) = 0.99526 \text{ \AA}$).

Table 3. Measured hyperfine splitting Δ^a (kHz) and residual o-c of DCO⁺, DNC, and HN¹³C relative to a selected hyperfine component. If no numbers are given for the value of a measured splitting and its residual, the hyperfine component overlaps with the previous component. The values of the splitting and the residual refer to the respective intensity weighted averages.

Transition	Splitting	Residual ^b
DCO ⁺ : $F = 2 - 1$ at 72039.306 (3) MHz		
1 - 1	+47.58 (144)	1.20
0 - 1	-64.64 (144)	0.80
DNC: $I, F = 2, 1 - 2, 2/2, 1 - 0, 0$ at 76305.512 (3) MHz		
1, 1 - 1, 1	115.30 (100)	-0.18
2, 3 - 2, 2	175.44 (100)	-0.72
1, 2 - 1, 1	204.63 (100)	1.38
2, 2 - 2, 2	277.57 (100)	-0.82
0, 1 - 0, 0		
0, 1 - 2, 2		
1, 0 - 1, 1	325.50 (250)	1.60
HN ¹³ C: $F_1, F_2, F = 0, 1, 1 - 1, 2, 2$ at 87090.675 (3) MHz		
2, 2, 2 - 1, 1, 1	115.5 (50)	-7.3
2, 2, 2 - 1, 2, 2		
2, 2, 1 - 1, 1, 0		
2, 2, 1 - 1, 2, 1		
2, 3, 3 - 1, 2, 2	158.5 (50)	5.0
2, 3, 2 - 1, 1, 1		
2, 3, 2 - 1, 2, 1		
1, 1, 1 - 1, 1, 1	210.7 (50)	1.5
1, 2, 2 - 1, 2, 1		
1, 2, 2 - 1, 2, 2		

^a Numbers in parentheses are one standard deviation in units of the least significant figures.

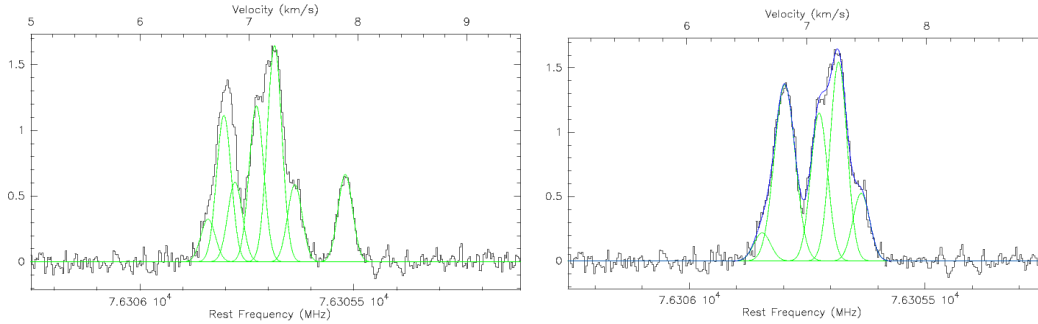
^b Residuals for DCO⁺ refer to fit with C_I kept fixed. The residuals are zero if C_I is released as two pieces of information are then used to derive two parameters.

Table 4. Derived hyperfine parameters^a (kHz) of DCO⁺ in comparison to previous experimental and present quantum-chemically calculated values.

Parameter	Value			
	This work	This work	Caselli & Dore (2005)	calculated
eQq	+150.00 (266)	+151.12 (288)	+147.8 (35)	+156.0
C_I	-0.69 ^b	-1.12 (43)	-1.59 (78)	-0.69

^a Numbers in parentheses are one standard deviation in units of the least significant figures.

^b Kept fixed in the analysis.

**Fig. 2.** Spectrum of the $J = 1 - 0$ transition of DNC toward the dark cloud LDN 1512, obtained with the IRAM 30m telescope. Vertical scale is antenna temperature (T_{mb}) in K. Left panel: Gaussian decomposition of the broad blended feature into six components which are assumed to have the same width as the single isolated feature. Right panel: Spectrum with the isolated feature subtracted and a reduced five-component fit to the remaining broad feature.**Table 5.** Hyperfine parameters^a (kHz) of DNC in comparison to previous experimental and present quantum-chemically calculated values.

Parameter	Value		
	This work	Bechtel et al. (2006)	ab initio
$eQq(\text{N})$	+288.2 (71)	+294.7 (131)	+309.6
$C_I(\text{N})$	+4.91 (63)	+5.01 (99)	+5.54
$eQq(\text{D})$	+265.9 (83)	+261.9 (145)	+257.6
$C_I(\text{D})$	-0.60 ^b	–	-0.60
$S(\text{ND})$	-1.35 ^b	–	–

^a Numbers in parentheses are one standard deviation in units of the least significant figures.

^b Kept fixed to computed values in the analysis.

Table 6. Hyperfine parameters^a (kHz) of HN¹³C in comparison to ab initio values.

Parameter	Value	
	experimental	ab initio
$eQq(\text{N})$	+272.5 (51)	+279.5
$C_I(\text{N})$	+6.33 ^b	+6.33
$C_I(^{13}\text{C})$	+23.46 ^b	+23.46
$C_I(\text{H})$	-4.49 ^b	-4.49
$S(\text{HN})$	-8.79 ^b	–
$S(\text{N}^{13}\text{C})$	-1.37 ^b	–
$S(\text{H}^{13}\text{C})$	-2.98 ^b	–

^a Numbers in parentheses are one standard deviation in units of the least significant figures.

^b Kept fixed to computed values in the analysis.

Table 7. Velocity offsets and intrinsic strengths of hyperfine components of the DCO⁺, DNC, and HN¹³C $J = 1-0$ lines.

Transition	Component	Offset km s ⁻¹	Relative intensity
DCO ⁺ $J = 1-0$	$F=0-1$	+0.269	0.20
	$F=2-1$	±0.0	1.00
	$F=1-1$	-0.198	0.60
DNC $J = 1-0$	$I, F=2,1-2,2 / 2,1-0,0$	±0.0	1.00
	$I, F=1,1-1,1$	-0.453	0.99
	$I, F=2,3-2,2$	-0.689	2.33
	$I, F=1,2-1,1$	-0.804	1.67
	$I, F=2,2-2,2 / 0,1-0,0 / 0,1-2,2$	-1.091	2.67
HN ¹³ C $J = 1-0$	$I, F=1,0-1,1$	-1.279	0.33
	$F_1, F_2, F=0,1,1-1,2,2$	±0.0	1.00
	$F_1, F_2, F=2,2,2-1,1,1 / 2,2,2-1,2,2 / 2,2,1-1,1,0 / 2,2,1-1,1,0$	-0.398	4.04
	$F_1, F_2, F=2,3,3-1,2,2 / 2,3,2-1,1,1 / 2,3,2-1,2,1$	-0.546	6.63
	$F_1, F_2, F=1,1,1-1,1,1 / 1,2,2-1,2,1 / 1,2,2-1,2,2$	-0.725	3.66